

Corrosion and Chloride Diffusivity of Reinforced Concrete Cracked under Sustained Flexure

Nilüfer ÖZYURT¹

Tayfun Altuğ SÖYLEV²

Turan ÖZTURAN³

Ahmet Onur PEHLİVAN⁴

Anıl NİŞ⁵

ABSTRACT

This research discusses the chloride diffusivity of concrete as well as corrosion performance of rebars in cracked and uncracked states. Prismatic concrete specimens with two water-to-cement ratios, two concrete cover thicknesses with and without steel fibers were used. Three-point flexural loading was applied to form cracks and cracks were sustained by a bolt system. Half-cell potential and corrosion rate measurements were carried out following wetting - drying cycles in chloride environment which were continued for 80 weeks. The positive effects of lower water-to-cement ratio and greater cover depth were found to be surpassed by existence of cracks in concrete.

Keywords: Corrosion, cracked concrete, corrosion rate, chloride profiles, diffusion coefficient, fibers, sustained crack width, sustained flexure.

1. INTRODUCTION

Corrosion is a major cause of deterioration for concrete structures. Especially chloride induced corrosion is one of the most severe of all corrosion mechanisms. Thus, penetration of chloride into concrete and chloride induced corrosion has been an important issue in the

Note:

- This paper has been received on June 4, 2018 and accepted for publication by the Editorial Board on May 30, 2019.
- Discussions on this paper will be accepted by January 31, 2021.
- <https://dx.doi.org/10.18400/tekderg.430536>

1 Boğaziçi University, Department of Civil Engineering, İstanbul, Turkey - nilufer.ozyurt@boun.edu.tr - <https://orcid.org/0000-0003-4533-8702>

2 Gebze Technical University, Department of Civil Engineering, Kocaeli, Turkey - tasoylev@gtu.edu.tr - <https://orcid.org/0000-0001-5042-0431>

3 Boğaziçi University, Department of Civil Engineering, İstanbul, Turkey - ozturan@boun.edu.tr - <https://orcid.org/0000-0001-8097-3838>

4 Maltepe University, Department of Civil Engineering, İstanbul, Turkey - onurpehlivan@maltepe.edu.tr - <https://orcid.org/0000-0002-6296-4126>

5 İstanbul Gelisim University, Department of Civil Engineering, İstanbul, Turkey - anis@gelisim.edu.tr - <https://orcid.org/0000-0001-9092-8088>

design of concrete structures and studied by several researchers [1-7]. Penetration of chloride ions into concrete destructs the passivation layer on the reinforcement and initiates the corrosion process. Corrosion of rebars degrades the performance of reinforced concrete structure by decreasing the cross-sectional area of reinforcement and deteriorating the bond between concrete and steel.

Previous research on corrosion of concrete has been conducted mostly on uncracked specimens however cracks in reinforced concrete structures are inevitable. In practice, concrete can crack due to several reasons and these cracks can alter the mechanism and duration of chloride penetration. Transportation of chloride ions in cracked specimens takes less time with respect to uncracked ones. Hence, it is very important to study the influence of cracks on the corrosion of rebars and chloride penetration in concrete. Effects of cracks on water, gas and chloride permeability have been investigated in several studies that led to controversial results and no clear conclusion can be derived. Effects of cracks on permeability of concrete were investigated in several studies and it was found that cracks affect the ingress of water into concrete [8-10].

In recent years, some researchers conducted chloride penetration tests on specimens with flexural cracks. Rodriguez and Hooton [1] studied the chloride ingress in artificially cracked concrete and concluded that cracks did not affect the diffusion coefficient. Win et al. [2] formed cracks on reinforced concrete specimens and exposed preloaded cracked specimens to chloride environment and concluded that cracks accelerated the penetration of chloride ions. Şahmaran [11] exposed preloaded cracked specimens at different crack widths to sodium chloride solution and concluded that specimens with crack widths lower than 0.135 mm had marginal chloride penetration where for the specimens with cracks larger than 0.135 mm diffusion coefficient increased rapidly. Marsavina et al. [3] used beam specimens with artificial cracks and concluded that cracked specimens showed higher chloride penetration in comparison with the uncracked specimens. In these studies, cracks were either artificial or loads applied to form cracks were removed after obtaining the intended crack width. Since structural members are under service loads at all times, removing the loads before exposing test specimens to aggressive environment may not represent the real situation. Sustaining the loads (to keep the crack open) may give more realistic results. Gowripalan et al. [4] used a ratio of crack width to concrete cover depth and studied the chloride diffusivity in the tension and compression zones of concrete cracked under sustained bending and found that the chloride diffusivity in the cracked tension zone was higher than the compression zone. Wang et al. [12] studied the chloride transport in concrete under sustained loads and concluded that chloride diffusivity decreased in the compression zone, while increased in the tension zone of the specimens. An increase in surface crack width from 0.05 mm to 0.20 mm caused a significant increase in the chloride content of concrete [13]. Crack width played a dominant role in chloride transport in cracked concrete (for transverse crack width up to 0.4 mm) together with the concrete quality [14].

Considerable amount of research was also conducted on the effects of cracks on reinforcement corrosion. Beeby [15] reported that effect of cracks loses its significance in long term. Also, in some other studies, effects of cracks were found to be small after the corrosion initiation period [5, 16]. In a study of Mohammed et al. [17], authors found that cracks that occurred under flexural loading increased the oxygen permeability of concrete cover and the oxygen concentration at the reinforcement level and thus increased the risk of

corrosion. In another study of Mohammed et al. [18], authors concluded that cracks increased the risk of corrosion, yet effect of crack width was lower than the effect of water-to-cement ratio. Most studies in literature are on the chloride penetration into saturated concrete. However, in reality concrete was found to be unsaturated, especially when it was subjected to wetting-drying cycles [19].

The results of the research study carried out by Otieno et al. suggested that for a given concrete quality (binder type and w/b ratio) and cover depth, corrosion rates increased with increase in crack width (w_{cr}) in the order: uncracked < 0.4 mm cracked < 0.7 mm cracked under chloride exposure. However, corrosion rate at a given crack width varied depending on the cover depth (20 mm and 40 mm) and concrete quality. For a given concrete cover thickness-to-surface crack width ratio (c/w_{cr}), corrosion rates varied significantly depending on the concrete quality [20]. The effect of the c/w_{cr} ratio was also reflected to the findings of Lu et. al, which showed an average loss in the diameter of steel bar in concrete with 0.2 mm crack more than twice as high as that of the uncracked concrete for 20 mm cover thickness, whereas there was only a slight increase in the loss of diameter for 40 mm cover thickness. According to the study, when the crack width was less than 0.1 mm, it did not affect the corrosion [14]. On the other hand, the study of Berrocal et al. indicated that after a period of 120 days chloride exposure, the specimen with 0.1 mm crack width started to corrode, while the uncracked specimens showed no sign of corrosion after 200 days of cyclic chloride exposure [21]. The shorter corrosion initiation time in the presence of transverse crack width smaller than 0.1 mm was reported by other studies. These studies found also higher corrosion rate results in the specimens with low crack width, which were supported by the visual observation of the steel surface [22-23]. Sangoju et al. concluded that the presence of the crack influences corrosion more than the crack width itself as mentioned also in another study [23], when they found that the increase in weight loss between the uncracked to 0.2 mm crack-width specimens was higher than between the 0.2 and 0.4 mm crack-width specimens. The weight loss for both uncracked and precracked specimens of plain concrete was in the range of 11.9–22.4%, 13.9–25.2%, and 18.5–33.4%, respectively for w=c of 0.37, 0.47, and 0.57. It is interesting to note that, the mass loss in the highest quality but cracked concrete is higher than that in the lowest quality but uncracked concrete [24]. The increase in crack width shortened the corrosion initiation time [21] and significantly affected the corrosion rate [23] varying from 0.1 mm to 0.4 mm and from 0.1 to 1.0 mm, respectively.

Steel fibers are mainly used for enhancing the mechanical behavior of concrete structures. However, in addition to mechanical strength, durability properties of steel fiber reinforced concrete should also be investigated for better evaluation of the performance of the concrete structures. Studies focusing on the corrosion of steel fiber reinforced concrete are very limited. Granju and Balouch agreed that corrosion arising from cracks is less severe when steel fibers are used [25]. However, as stated by other researchers [26] contradictory results exist on the use of fibers in chloride environments together with reinforcing bars. Therefore, further research on the subject is needed. The use of steel fibers provided a slight reduction in the corrosion initiation time for reinforcing steel embedded in cracked concrete (0.1 mm - 0.4 mm) under chloride exposure. However, there was significant improvement in corrosion resistance by the use of PVA fibers and hybrid fibers (steel + PVA) [21]. According to the results of another study, there was no significant difference in terms of corrosion resistance measured by the gravimetric loss in the concrete with hybrid fibers (steel + PVA) with respect to the plain concrete [27].

From the above studies, it is understood that concrete cover thickness and quality are important parameters when chloride ingress into concrete is considered. However, in reality under service loads cracks can occur thereby altering the situation into a more complicated state about the parameters affecting corrosion of rebars. In this study, a more realistic approach to the exact situation of reinforced concrete structures was investigated in order to understand the effect of different parameters (cracks, fiber inclusion, concrete cover depth and quality). Cracks were formed and kept open under sustained loads. Crack widths were 0.4 mm for non-fibrous specimens, while they varied between 0.22 – 0.34 mm for fibrous specimens. Maximum allowable crack width values from 0.1 to 0.4 mm were given in different standards/guidelines (ACI 224.01 [28], ACI 318-08 [29]) in the last decades. Comparative tables were prepared by different researchers to analyze approach of several standards/countries [4,11,30]. Unfortunately, there is still no consensus on the acceptable crack width values. The limits defined in the standards maybe useful while designing new structures. However, the studies carried out on the existing structures showed that cracks with much greater widths than mentioned in the guidelines are encountered in the concrete. Baah [31] carried out a study on the slabs of 13 structural bridges in Ohio and prepared a table to represent recorded maximum crack widths. He stated that cracks from 0.7 mm to 3.3 mm were measured under dead load only. A crack width as great as 3.3 mm means a direct passage to reinforcement, even for very large cover depths. Considering such findings, a relatively high maximum crack width value (0.4 mm) was selected for this study. Specimens were exposed to severe chloride environment (3.5 % NaCl solution) by applying wetting-drying cycles for 80 weeks and weekly corrosion data (half-cell potential and corrosion rate) were recorded. After the exposure duration, chloride diffusion profiles were obtained and chloride diffusion coefficients were estimated. Also, images of corroded rebars were taken and analyzed for the compatibility of the results with each other.

2. EXPERIMENTAL STUDY

2.1. Materials and Mix Design

Type I Portland cement (CEM I 42.5 R), two types of coarse aggregates ($D_{max} = 20\text{mm}$) and crushed as well as local river sand were used in making the concretes. ASTM C494 type F high range water-reducing superplasticizer (naphtalene based) was added to achieve a slump of about 17 ± 2 cm. Hooked end steel fibers of 0.55mm diameter and 35 mm length (length/diameter ratio=65) with a tensile strength of 1100 MPa were used in fibrous specimens.

Two water-to-cement ratios (0.45 and 0.65) and two different concrete cover depths (25 mm and 45 mm) were used with and without fibers. Details of the mix proportions are given in Table 1.

Eight series of concretes were produced to cast 64 concrete prisms (100 x 100 x 500 mm) with reinforcing bars. Specimens were cast in two layers and compacted using a vibrating table. After casting, specimens were covered with plastic sheets to prevent evaporation of mix water. Prisms were demolded after 24h and cured in moist room at 23 ± 2 °C for 28 days. Three cylinder specimens with a diameter of 100 mm and a height of 200 mm were also cast from each series for compressive strength testing.

Table 1 - Mix proportions of concrete.

Mixes	w/c	Mix proportions (kg/m ³)					
		Cement	Water	Sand	Coarse Aggregate	Steel Fiber	SP
F065	0.65	310	201	797	1054	0	2.22
F045	0.45	400	180	797	1043	0	6.30
F165	0.65	310	201	797	1054	39	3.48
F145	0.45	400	180	797	1043	39	6.85

Following notation was used for designation of the specimens. F1 and F0 stand for the specimens with and without fibers. The following numbers, 45 and 65 show the water-to-cement ratio of the specimens, 0.45 and 0.65, respectively. The last two digits indicate concrete cover thickness of 25 mm and 45 mm. Thus, F14525 represents concrete with fibers, cast by using a w/c of 0.45 and a cover thickness of 25 mm.

2.2. Mechanical Tests

- **Compressive strength tests**

Compressive strength tests were performed according to ASTM C39 [32] on 100 x 200 mm cylinders at the age of 28 days.

- **Evaluation of force vs. crack width relation (preliminary experiments)**

Three-point bending tests were conducted to create the maximum possible crack width and to determine the ultimate flexural capacity of the reinforced concrete prisms in order to see also whether or not a 0.4 mm crack width can be achieved for all the specimens (Figure 1).

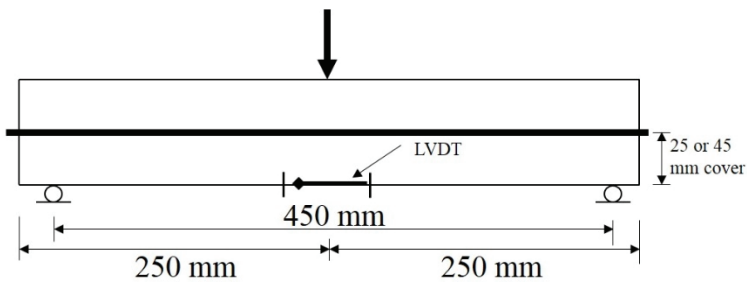


Figure 1 - Three-point bending test set-up

- **Sandwich cracking of specimens**

Each concrete prismatic specimen was reinforced with a 14 mm hot-rolled ribbed bar with a characteristic yield strength of 420 MPa as was stated above. The rebars were extended

beyond the concrete at both ends, in order to make corrosion measurements effectively. In order to sustain flexural loads on the prisms and prevent the closing of cracks, a set-up depicted in Figure 2 was used. As illustrated in Figure 2, a dummy specimen with identical properties was used for creating similar bending rigidity (32 dummy specimens were cast total, 4 specimens were used for each series). A smooth steel rod was placed between the dummy and the test specimens in the test setup in order to create compression and tension stresses on the inner and outer sides of the specimens, respectively. The system was loaded under stroke displacement control. Loading was applied at a rate of 0.001 mm/sec. When the crack width of 0.4 mm was achieved, bolts were tightened to sustain the load on the specimen and eventually the width of the crack. Two LVDTs were placed on both sides at the midsection of the tension zone of the test specimen as can be viewed from Figure 2 to measure the crack width. Specimens without fibers were cracked at mid-span to a crack width of 0.4 mm. Flexural loads needed to open the crack to a width of 0.4 mm were recorded. Fibrous specimens were loaded up to the pre-recorded flexure loads (for non-fibrous specimens) by using the same set-up, and the corresponding crack widths were recorded.

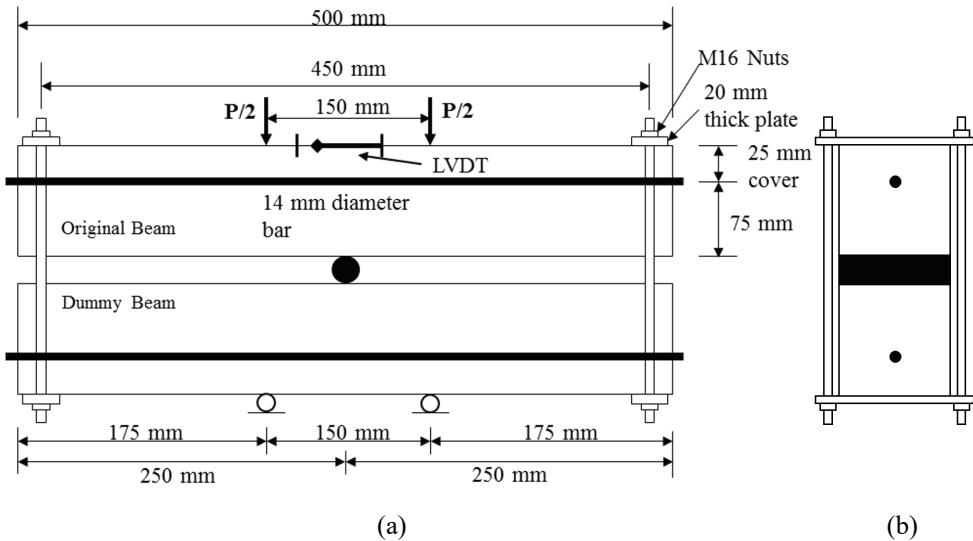


Figure 2 - Schematic diagram of the test setup ((a) front view and (b) side view).

2.3. Exposure Conditions

After cracking process, 70x130x15 mm reservoirs were made on the cracked face of each test beam by using silicon and a cement-based material for waterproofing. A 35g/l NaCl solution was used to expose the specimens to repeated cycles of 4 day ponding followed by 3 day air drying period. These cycles were continued for 80 weeks for the cracked and uncracked specimens. Cracked specimens were under sustained loading during exposure. Temperature and relative humidity of the storage area were measured and noted at certain intervals.

2.4. Corrosion Monitoring

Two different corrosion assessment techniques were used. Corrosion measurements were made in accordance with ASTM C876 [33] by galvanostatic pulse technique with an Ag/AgCl electrode (SSCE) measuring both corrosion rate and half-cell potential at the same time. A short time anodic current pulse is applied to reinforcement galvanostatically from a counter electrode placed on concrete surface together with a reference electrode. With the applied current, reinforcement gets polarized in the anodic direction compared to its free corrosion potential. A reference electrode which is placed in the center of the counter electrode record the resulting change of the electrochemical potential of the reinforcement as a function of polarization time.

Half-cell potential and corrosion rate measurements began 10 weeks after exposure due to a breakdown in the galvanostatic pulse device. In order to compensate for the missing data, new series of concrete specimens were cast and tested in uncracked state (3 specimens for each series). The comments on the results obtained from later produced uncracked specimens will be given in results and discussion section.

For half-cell circuit, it can be said that a certain decrease in the half-cell potential of the rebar can be correlated with the time to depassivation whereas corrosion rate is related to the loss of reinforcement cross-section. While half-cell measurements give information about corrosion initiation time, corrosion rate measurements are used to evaluate overall life time performance of rebars. Therefore, corrosion rate results are used as one of the most significant input parameters in corrosion-induced damage prediction models for reinforced concrete structures.

2.5. Chloride Content Measurements

Chloride ion profiles and diffusion coefficient of concrete were evaluated in accordance with ASTM C1556 [34]. There are several chloride transport mechanisms that can take place in concrete. These are a) diffusion under the influence of a concentration gradient, b) absorption due to capillary suction, c) migration in an electric field, d) pressure induced flow and e) wick action when water absorption and water vapor diffusion are combined [6].

The transport mechanism occurring in the case of chloride ingress into concrete is diffusion under the influence of a concentration gradient. The transport of the chloride ions into concrete specimens under sustained loading is assumed to be one dimensional in a semi-infinite medium complying with Fick's second law of pure diffusion given as,

$$\frac{\partial C}{\partial t} = D \frac{\partial^2 C}{\partial x^2} \quad (1)$$

Where C = chloride concentration in concrete; t = exposure time, D = chloride diffusion coefficient and x = distance from surface.

An analytical solution to Equation 1 can be given by:

$$C(x, t) = C_s \left[1 - \operatorname{erf} \left(\frac{x}{2\sqrt{Dt}} \right) \right] \quad (2)$$

Where $C(x, t)$ is the chloride ion concentration at depth x after exposure time t for a chloride concentration of C_s at the concrete surface and the expression erf is the Gaussian error function.

Apparent chloride diffusion coefficient, D , and surface concentration, C_s , were determined by fitting the Equation 2 to the measured chloride contents by a non-linear regression analysis using the method of least squares. In the analysis of the chloride profile, the sum of the squared differences between the fitted and the actual data for the chloride-ion content of each sample must be minimized by adjusting the regressor variable [6]. Initial chloride content that may come from the mix ingredients can be neglected (if materials used are carefully controlled) in analyzing the chloride profiles [34]. Surface chloride content, C_s , is difficult to determine since chloride content at concrete surface is reduced due to several reasons. This is why C_s values were determined by fitting Equation 2 as suggested in the literature.

After completion of wetting - drying cycles for 60 and 80 weeks, the specimens were unbolted to be released from suspended load and measurements of chloride contents at different depths of concrete were done using the following procedure. First, powder samples from different depths of concrete specimens were collected by a profile grinder machine. Grinding process was carefully done by appropriate devices starting from the outmost layer exposed to NaCl solution going into deeper layers with intervals of 0-5 mm, 5-10 mm, 10-15 mm, 15-20 mm, 20-30 mm, 30-40 mm from concrete surface to the steel bar, pulverizing concrete into powder and handling carefully without any contamination. Second, chloride content of powder sample obtained from each layer was determined by acid soluble extraction in a nitric acid solution which was treated against 0.05 N silver nitrate (AgNO_3) by potentiometric titration within the requirements and precision levels given in ASTM C1152 [35]. Then, chloride content of each solution was calculated as percentage by weight of concrete. Finally, these results were used to create chloride profiles to determine diffusion coefficients (D) and surface concentrations (C_s).

3. RESULTS AND DISCUSSION

3.1. Fresh Concrete Properties

All concrete mixes were cast to achieve a slump of 17 ± 2 cm as mentioned before. Slump, air content and density measurements were done for all mixes. Resulting fresh concrete properties can be seen in Table 2.

3.2. Mechanical Properties

3.2.1. Compressive Strength Analysis

Compressive strengths of 100 x 200 mm cylindrical specimens were determined at the age of 28 days by applying compressive axial load at a rate of 4.8 kN/sec. Compressive strength of concretes as average of 3 specimens can be seen in Table 2.

Table 2 - Fresh state and compressive strength tests results

Mixes	w/c	Slump (cm)	Air Content (%)	Density (kg/m ³)	f _c (MPa)
F065	0.65	17.5	3.5	2250	29.8
F045	0.45	17.0	3.8	2320	49.0
F165	0.65	17.5	5.2	2300	28.1
F145	0.45	17.0	4.8	2360	47.9

3.2.2. Flexural Strength Analysis

Flexural tests were done to obtain failure load and crack width that can be achieved as explained in experimental study section. A crack width of 0.4 mm was selected as the critical crack width in this study. Figure 3 (a) and (b) show force vs. crack width relations for the specimens with cover depths of 45 mm and 25 mm, respectively.

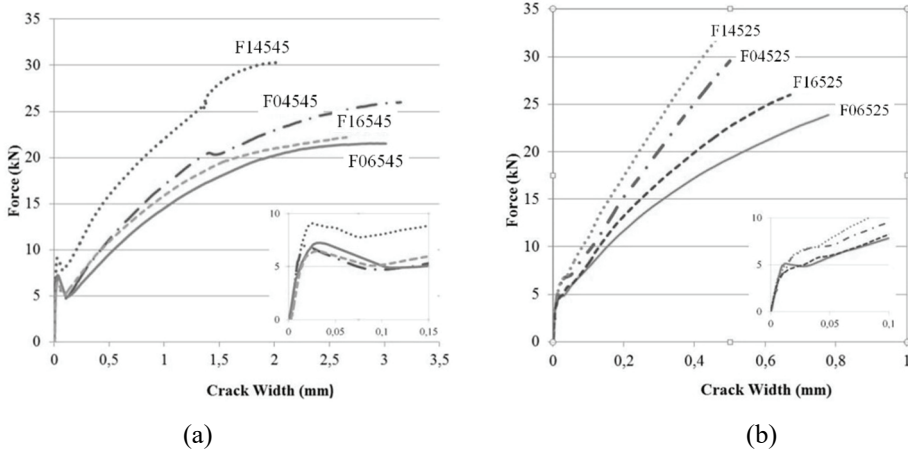


Figure 3 - Force vs. crack width relations of the specimens with a cover thickness of (a) 45 mm and (b) 25 mm

First cracking behavior of concrete is given in the onset of Figure 3 (a) and (b). Following the first cracking, deformations increased at a decreased stress level and after that the effect of steel reinforcement was seen (increased bending capacity of the section) for the higher cover thickness. In other words, there is a transition phase from plain concrete to reinforced concrete. Fiber presence can easily be identified with additional flexural capacity especially in higher quality concretes (w/c = 0.45). Specimens with 25 mm cover depth had less than 1 mm crack widths until failure while specimens with 45 mm concrete cover depth had three times higher crack widths before failure occurs. The flexure tests showed that it was possible to create selected critical crack width of 0.4 mm for all specimens.

3.2.3. Formation of Cracks under Sandwich Loading

In order to attain and keep the needed crack widths, sandwich test procedure was used as explained before in experimental study section. The procedure was applied to two specimens of each mixture. On non-fibrous specimens, cracks with a width of 0.4 mm were formed and maintained on test specimens as explained before. Load values required to form 0.4 mm cracks for these non-fibrous specimens were recorded and then applied to the fibrous specimens and the cracks formed were measured and maintained.

The reason for applying the load required to form 0.4 mm crack on non-fibrous specimens to fibrous specimens was to see the contribution of fibers on crack width bridging. So as previewed from flexural test results, fibrous specimens showed the ability to attain smaller crack widths under same load levels (Figure 4).

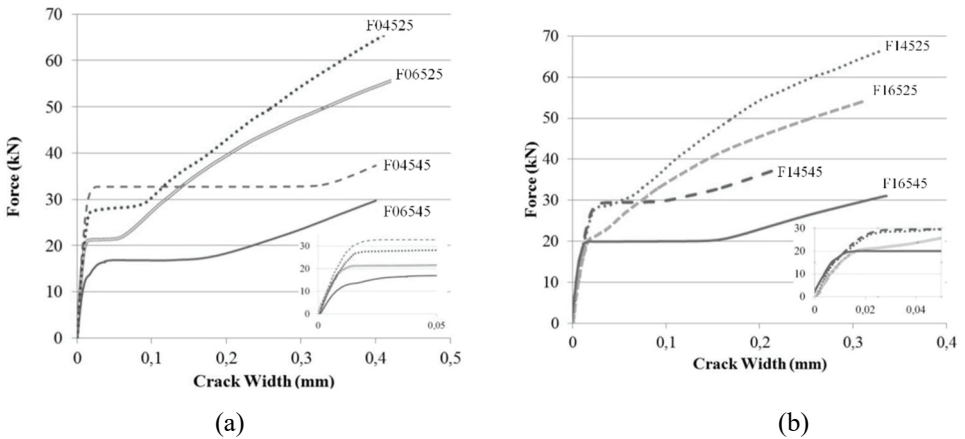


Figure 4 - Force - crack width diagrams of specimens (a) without fibers and (b) with fibers.

It can be seen from Figure 4 that all fibrous specimens had smaller crack widths than their control specimens. This can be an early advantage for fibrous specimens before starting wetting - drying cycles. All cracks on the specimens were examined by naked eye and a magnifier (x10) and it was observed that there were one large and some very small distributed cracks on the specimens.

3.3. Corrosion Results

Corrosion tests were conducted for both cracked and uncracked specimens. Half-cell potential and corrosion rate measurements by using a galvanostatic pulse device were carried out for corrosion monitoring. For the first 60 weeks, 2 cracked specimens and 3 uncracked specimens were used. At the end of the 60 weeks period, 2 specimens (1 cracked and 1 uncracked) of each series were used for chloride content determination. Corrosion tests were continued until 80th week and again 2 specimens (1 cracked and 1 uncracked) of each series were used for chloride content determination.

• **Half-cell potential measurements**

Figure 5 and Figure 6, represent the half-cell potential values for uncracked and cracked specimens, respectively. The effects of various factors are seen when figures are examined. The results are interpreted based on limit values given in Table 3. The regions representing low and high risk of corrosion occurrence are separated for the attention of the readers.

Table 3 - Interpretation of half-cell potential values (ASTM C876 [33] /ASTM G3 [36])

Ag/AgCl (SSCE)	Interpretation
$E > -83\text{mV}$	Greater than 90% probability that no corrosion is occurring.
$-233\text{mV} < E < -83\text{mV}$	Corrosion activity is uncertain.
$E < -233\text{mV}$	Greater than 90% probability that corrosion is occurring.

The positive effects of water-to-cement ratio and cover thickness are easily seen in uncracked specimens (Figure 5). However, when Figure 5 is examined, it is seen that the advantage of using higher cover thickness is significantly decreased for cracked specimens. This is expected since the time needed for aggressive agents to penetrate into concrete to reinforcement decreased almost to zero when concrete cover was cracked. It should be emphasized that concrete was not only cracked but also under sustained loading, which resulted in a minimum crack width of approximately 0.22 and 0.40 mm for fibrous and non-fibrous specimens, respectively, for all times. The visual observations showed that, the crack directly went down to rebar when the crack widths given above were reached. The effect of water-to-cement ratio on half-cell potential results may also be considered secondary when concrete cover was cracked, since direct passage of aggressive agents to steel rebar was possible through the crack.

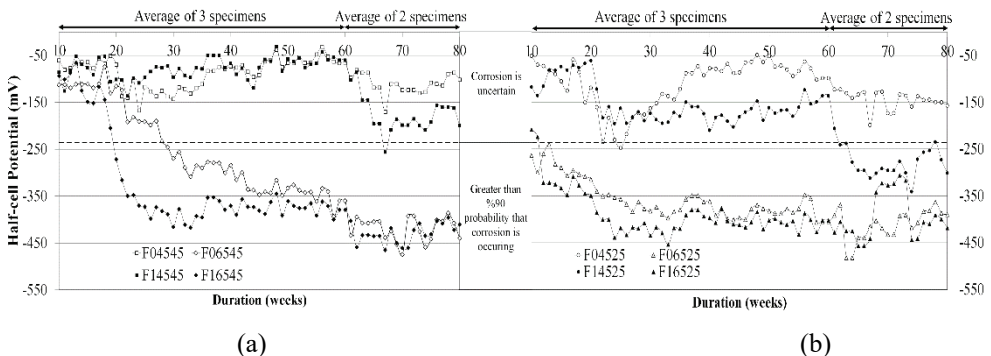


Figure 5 - Half-cell potential values of uncracked specimens with a cover depth of (a) 45 mm, (b) 25 mm

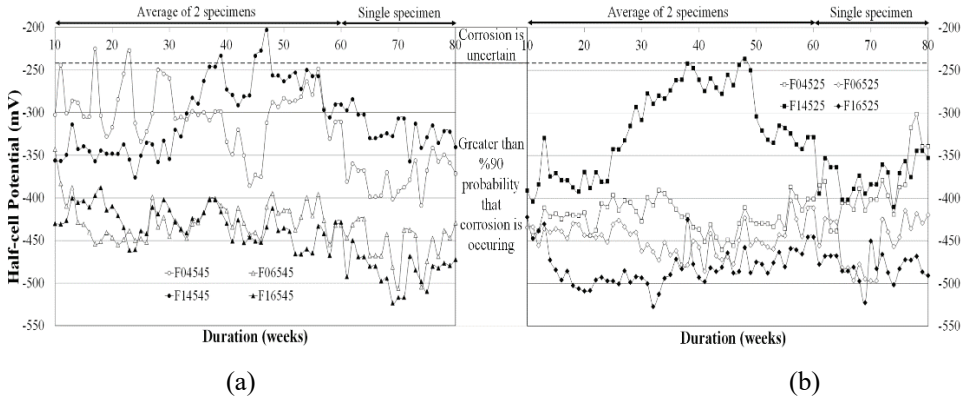


Figure 6 - Half-cell potential values of cracked specimens with a cover depth of (a) 45 mm, (b) 25 mm

It was observed that fibrous specimens yielded higher probability of corrosion occurrence especially in the uncracked state and this effect was more pronounced for low water-to-cement ratio specimens. This behavior may be explained by the existence of extra pores in fibrous specimens. Air contents of all mixes were measured by using pressure method immediately after mixing and the results showed that air contents of the fibrous mixes were higher when compared to non-fibrous mixes (Table 2). The expected positive effect of fibers was seen in the cracked state (Figure 6) for the specimens with low water-to-cement ratio (w/c : 0.45). Unfortunately, the same effect was not seen for high water-to-cement ratio specimens (w/c : 0.65). It is hypothesized that the positive effect of smaller crack width is reduced by the high permeability of the matrix.

Half – cell potential values are generally correlated with the time to depassivation as mentioned in Section 0. This gives an idea about corrosion initiation time for the specimens. Corrosion measurements began 10 weeks after exposure due to a breakdown in the galvanostatic pulse device as was mentioned in Section 0. A new series of uncracked specimens were cast and exposed to same wetting - drying cycles and the same corrosion monitoring procedure was applied to control the consistency of data obtained from the equipment. Results very similar to the data given in Figure 5 were obtained.

Based on the results, given in Figure 5 and obtained from latter produced specimens, corrosion initiation was not observed for the uncracked specimens produced using low water – to – cement ratio (0.45) at the end of 80 weeks of exposure (uncertain corrosion based on Table 3). However, corrosion initiation was observed earlier (from 10th week) on the rebars inside the uncracked specimens cast by using high water – to – cement ratio. For cracked specimens no extra specimens were cast since measurements showed corrosion initiation in the first 10 weeks. Therefore, corrosion was assumed to initiate immediately after NaCl exposure (based on very low half-cell potential values given in Figure 6). Later, the rebars were extracted from concrete specimens for visual examination of corrosion and for comparative checking of half-cell potential results.

4. CORROSION RATE MEASUREMENTS

Results of corrosion rate measurements are given in Figure 7 to Figure 10. The test results are presented separately for all mixtures for easy visualization by the readers. Corrosion rates were interpreted using Table 4 which was given by Frolund et al. [37]. Although, no standard table exists to interpret the corrosion rate data, Table 4 is found to be useful for evaluating the data obtained by using the equipment employed in this study. In evaluating the corrosion rate data, it should be kept in mind that the number of specimens dropped from 3 to 2 for the tests from 60 to 80 weeks. Therefore, degree of freedom in the data is decreased.

Table 4 - Interpretation of corrosion rate results [37].

I_{corr}	Interpretation
$< 0.5 \mu A/cm^2$	Passive Areas
$0.5-2 \mu A/cm^2$	Negligible corrosion activity
$2-5 \mu A/cm^2$	Low corrosion activity
$5-15 \mu A/cm^2$	Moderate corrosion activity
$>15 \mu A/cm^2$	High corrosion activity

Corrosion rate measurements of uncracked specimens are seen in Figures 7 and 8. Corrosion rates significantly increased when water-to-cement ratio was increased. No significant effect of fibers was observed on corrosion rate measurements of uncracked specimens.

The corrosion rate results of cracked specimens are given in Figures 9 and 10. The effect of water-to-cement ratio was important but less pronounced compared to uncracked specimens. Again, the effect of cover thickness was not pronounced. However, the effect of using fibers was more significant when concrete was cracked, since the crack opening is limited by fibers.

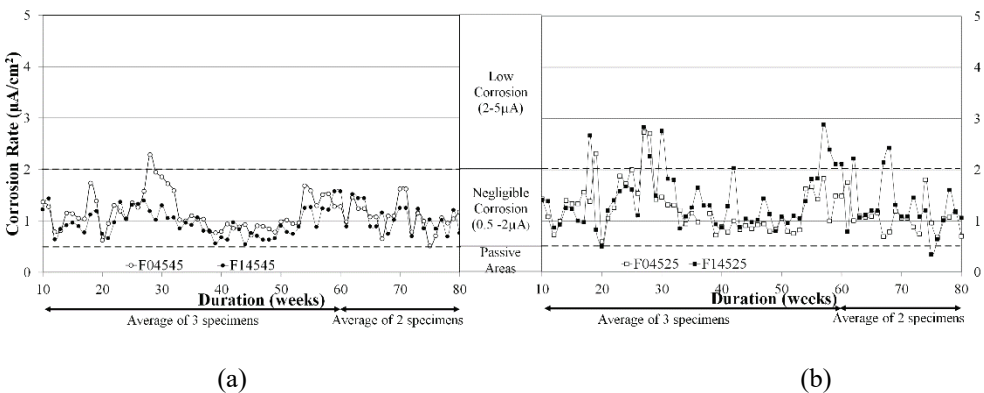


Figure 7 - Corrosion rates of uncracked specimens with w/c ratio of 0.45 and a concrete cover of (a) 45 mm (b) 25 mm

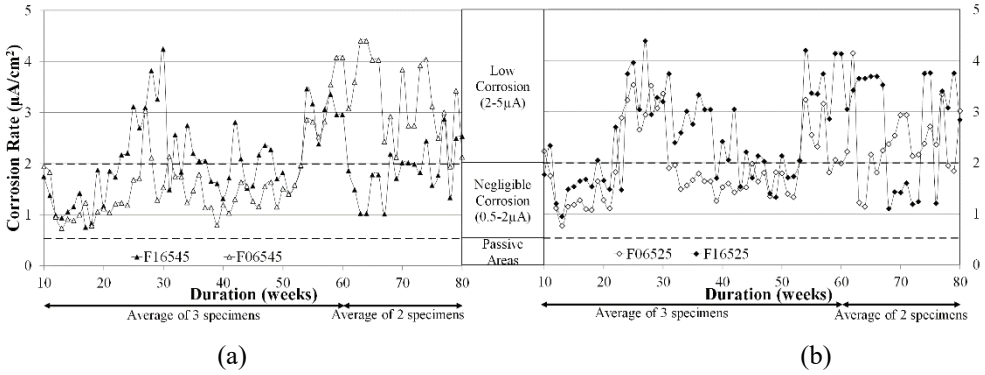


Figure 8 - Corrosion rates of uncracked specimens with w/c ratio of 0.65 and a concrete cover of (a) 45 mm (b) 25 mm.

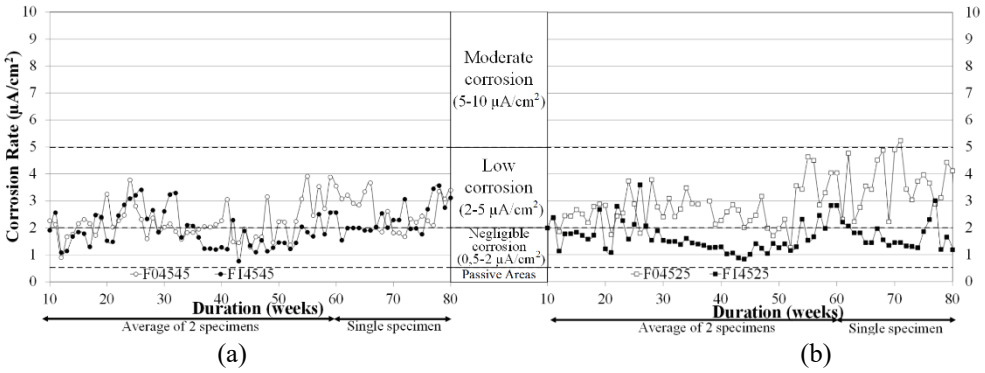


Figure 9 - Corrosion rates of cracked specimens with w/c ratio of 0.45 and a concrete cover of (a) 45 mm (b) 25 mm.

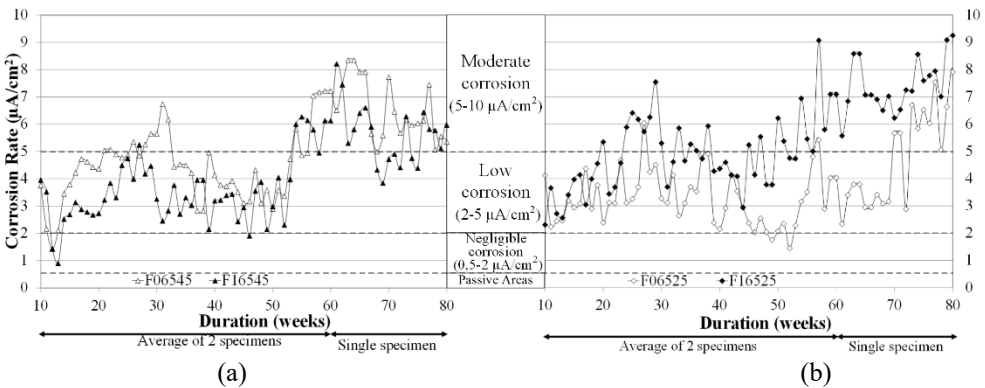


Figure 10 - Corrosion rates of cracked specimens with w/c ratio of 0.65 and a concrete cover of (a) 45 mm (b) 25 mm.

4.1. Chloride Penetration Results

Chloride penetration tests were conducted for all specimens at the end of wetting-drying period as explained in Section 0.

- Chloride Profiles

Chloride profiles of the specimens that were exposed to wetting-drying cycles for 80 weeks were given separately in Figure 11 - Figure 13.

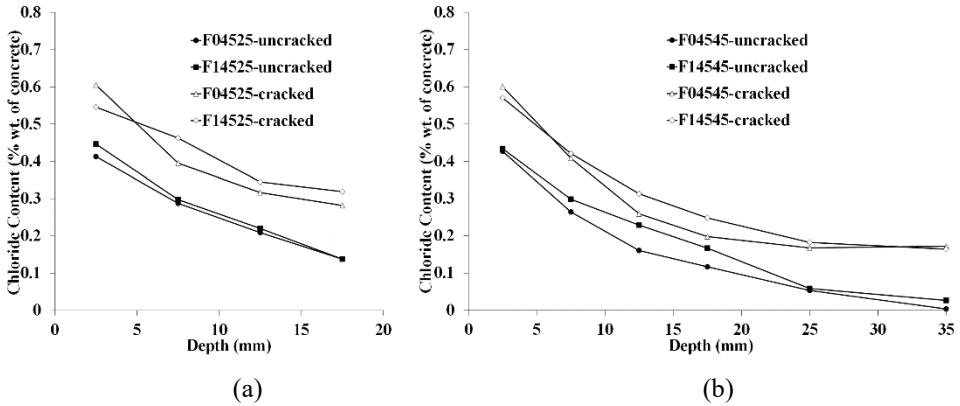


Figure 11 - Effect of cracks and fibers on chloride penetration of specimens with a w/c ratio of 0.45 and a concrete cover of (a) 25 mm (b) 45 mm (after 80 weeks of exposure).

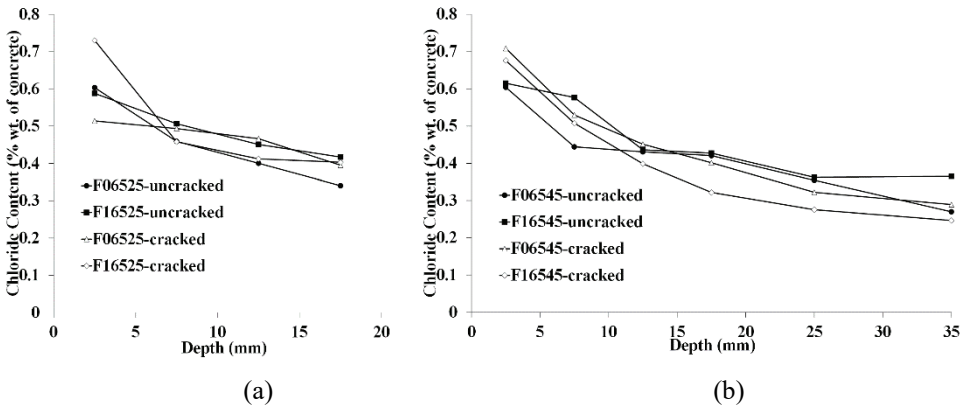


Figure 12 - Effect of cracks and fibers on chloride penetration of specimens with a w/c ratio of 0.65 and a concrete cover of (a) 25 mm (b) 45 mm (after 80 weeks of exposure)

It was observed that cracks were more effective in increasing the diffusion of chloride ions at low water-to-cement ratio (0.45) concretes (Figure 11). However, the same effect was not

seen when water-to-cement ratio was increased to 0.65 (Figure 12), which was due to more porous microstructure of the high water-to-cement ratio concrete. Cover depth was found to be effective when low water-to-cement ratio mixes (0.45) were used (Figure 11). Chloride contents close to zero were observed for the uncracked specimens with a cover depth of 45 mm after 80 weeks of exposure. Same result was not valid for high water-to-cement ratio mixes. The effect of cover depth was almost negligible for high water-to-cement ratio mixes (0.65) even for uncracked specimens probably due to high permeability of concrete (Figure 12).

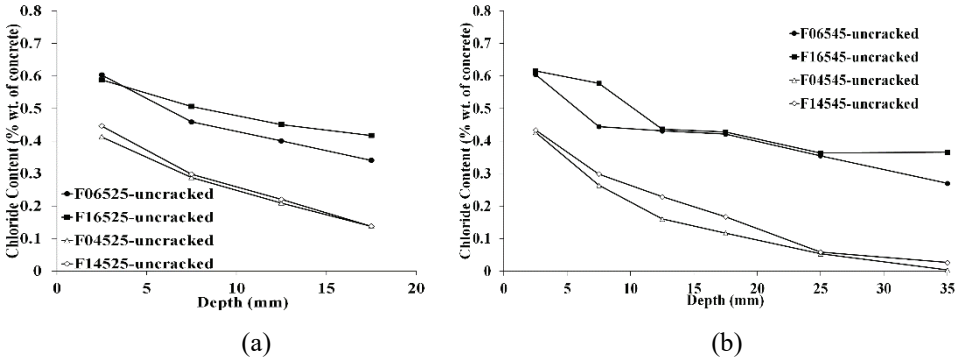


Figure 13 - Effect of water-to-cement ratio and cover depth on chloride penetration of uncracked specimens with a concrete cover of a) 25 mm b) 45 mm (after 80 weeks of exposure).

The chloride penetration data is presented in Figure 13 to indicate the effect of water-to-cement ratio and cover depth after 80 weeks of exposure of uncracked specimens. It was observed that the water-to-cement ratio was the most pronounced parameter as mentioned above. Chloride penetration was increased greatly with an increased water-to-cement ratio even in the uncracked state due to increased porosity and thus permeability of the concrete. Effectiveness of greater cover depth was also observed for 80 weeks of exposure of lower water-to-cement ratio concretes.

• **Diffusion Coefficients**

Diffusion coefficients and % chloride content values at the rebar level for all the specimens were predicted by using 2nd Fick’s law and given in Table 5.

As seen from the Table 5, diffusion coefficients and chloride contents are more compatible for uncracked specimens compared to cracked specimens. For the cracked specimens % chloride concentrations were found to be higher on top of the rebar; whereas surprisingly for some of the cracked specimens this high % chloride concentration values were not accompanied by high diffusion coefficients. This is probably because of the change of transport mechanism of chloride ions with the existence of cracks. Change of transport mechanism with formation of cracks was also mentioned by several other researchers [7,38].

Based on the results of this study and literature [7] it can be said that, calculating the diffusion coefficient by using Fick’s second law of diffusion may be misleading for cracked specimens since diffusion is not the only active mechanism for these specimens.

Table 5 - Diffusion coefficients and chloride concentrations on rebar level (calculated using Fick’s 2nd law).

		w/c : 0.45		w/c : 0.65		
Code		D (10 ⁻¹² m ² /s)	Cl cont. (% by weight of concrete)	Code	D (10 ⁻¹² m ² /s)	Cl cont. (% by weight of concrete)
Uncracked	F04525	2.80	0.060	F06525	7.51	0.222
	F04545	1.99	0.001	F06545	23.24	0.197
	F14525	2.56	0.056	F16525	17.20	0.328
	F14545	3.11	0.005	F16545	30.01	0.246
Cracked	F04525	4.14	0.134	F06525	32.18	0.356
	F04545	4.72	0.021	F06545	14.03	0.150
	F14525	7.39	0.205	F16525	6.12	0.221
	F14545	6.67	0.044	F16545	10.20	0.099

Therefore, using diffusion coefficient as the only parameter while analyzing the corrosion potential of cracked concrete specimens may be misleading since true diffusion can’t be observed in these specimens.

3.5. Visual Observation of Corrosion on Rebars

All of the rebars taken out of the specimens after 60 and 80 weeks of exposure were visually examined and surface images were taken. Images of rebars after 80 weeks of exposure are given below for comparing the experimentally obtained results (half cell potential, I_{corr}, C_s, D and concentration values) with the exact corrosion states of rebars (Figure , Figure 1). Following comments can be made if Figure 14 and Figure 1 are carefully examined.

For the specimens with a water-to-cement ratio of 0.45, experimental data obtained using galvanostatic pulse technique were found to be in accordance with the observations made on the rebars taken out of the specimens. If Figure is examined together with the experimental values given, it is seen that, based on the classification given by ASTM C876 [30], no signs of corrosion were observed on the specimens that represented half-cell potential values in the “uncertain corrosion activity zone” (uncracked specimens cast using a water-to-cement ratio of 0.45 – except F14525). The corrosion rate of these specimens was also found in the “negligible corrosion activity” zone when Table 4 is examined. For all of the cracked specimens, half-cell potential values were assessed in the corrosion occurrence zone (> 90%). Corrosion rates of these specimens were found in the “low corrosion activity zone” except

F14525. In compliance with this result some corrosion was observed on all of the rebars taken out of these specimens except F14525.

For the specimens with a water-to-cement ratio of 0.65, again comparable results are seen between the corrosion observations and the experimental data. Corrosion activity was found on different parts of the rebars (as can be seen on the figure) and this is attributed to the high permeability of concrete. It is hypothesized that the solution may be diffused through different parts of concrete resulting in corrosion. It should be emphasized that only a part of the rebar beneath the ponding area was monitored for corrosion rate measurements. It is seen from the figure that this method of measurement, may be misleading for high permeability concretes, since harmful substances may diffuse through different parts of concrete resulting in corrosion on the regions which are not monitored. This phenomenon was observed on almost all of the uncracked specimens cast by using w/c of 0.65. This was not an issue for the cracked specimens, since solution directly reached to the rebar through the crack.



Figure 14 - Images of corroded rebars taken out of specimens with a water-to-cement ratio of 0.45.

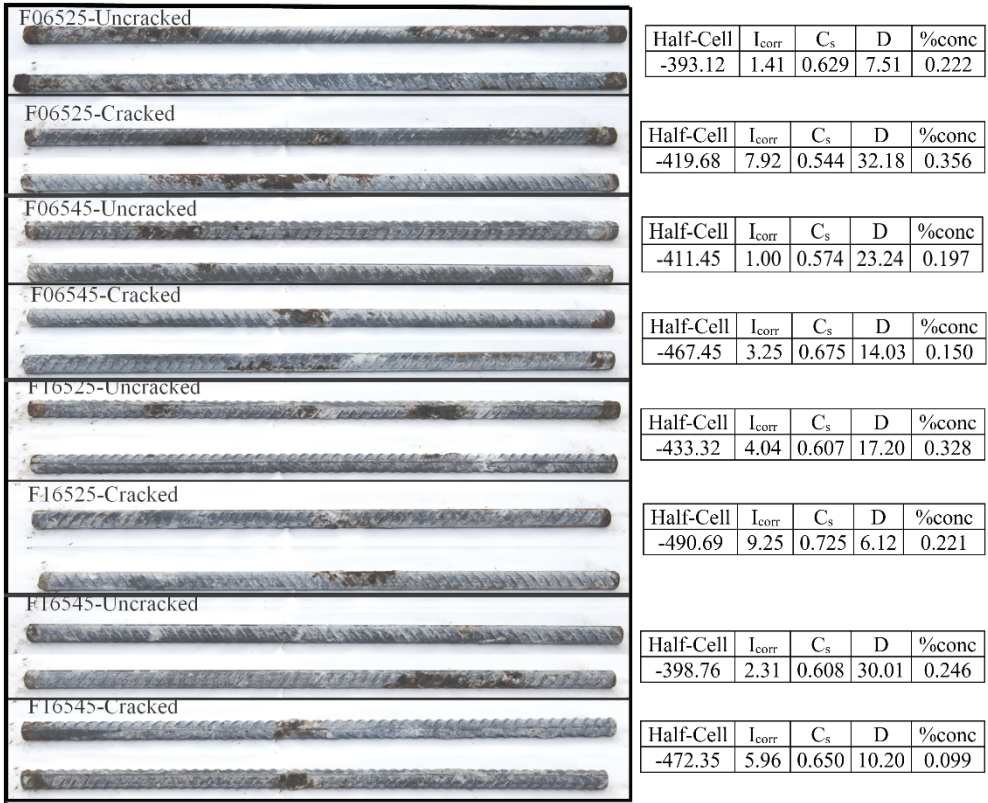


Figure 15 - Images of corroded rebars taken out of specimens with a water-to-cement ratio of 0.65.

5. CONCLUSIONS

Following conclusions were drawn from this comprehensive experimental study on the effects of chloride-induced corrosion on cracked and uncracked reinforced concrete.

1. Water-to-cement ratio was found to be the most effective parameter in the uncracked state. No corrosion was measured or observed on the rebars extracted from the specimens cast using a water-to-cement ratio of 0.45 after 80 weeks of exposure. Corrosion was found to initiate from 10-20 weeks for the uncracked specimens with high water-to-cement ratio of 0.65.

2. The positive effect of low water-to-cement ratio decreased in the cracked state. NaCl solution might have directly reached to the rebar through the open crack (0.3-0.4 mm) surpassing concrete cover resulting in an immediate corrosion initiation.

3. Increased cover depth was effective only for concretes with low water-to-cement ratio in the uncracked state. Increasing cover depth was not effective in reducing the rate of corrosion in high water-to-cement ratio and cracked concretes.

4. Fibers were not effective in the uncracked state where slightly higher corrosion was even observed, most probably due to higher air content measured in the fibrous specimens.
5. Positive effects of fibers were seen in the cracked concretes for low water-to-cement ratio mixes. No clear effect was observed when high water-to-cement ratio mixes were used.
6. Chloride contents (%) and diffusion coefficients were compatible for uncracked specimens which was not the case for cracked specimens. Diffusion is not the dominating mechanism for cracked concretes, where cracks are providing direct passage to the rebar for harmful substances.
7. Visual observations were in accordance with the results obtained from half-cell potential and corrosion rate measurements, except for the uncracked specimens with high water-to-cement ratio which showed corrosion on different parts of the rebar instead of the monitored ponding area (middle section). Chloride containing solution might have easily diffused in all directions through the material owing to high permeability of the matrix resulting in corrosion on different parts of rebars. However, this was not represented by corrosion rate measurements since only middle section of the rebar was examined in the scope of the test.
8. There is no agreement on the maximum allowable crack width in the standards. The results of this study showed how the protection provided by low water-to-cement ratio and high cover depth is to be questioned when crack widths up to 0.3 to 0.4 mm exist on the concrete surface. This implies the importance of having a concrete surface free from cracks and/or the regular control/maintenance procedures of concrete surfaces for protection against corrosion.

Acknowledgement

The authors gratefully acknowledge the financial support of TUBITAK (110M-264). They also would like to thank to AKÇANSA Cement, BASF-YKS Construction Chemicals and LIMAK Construction for providing materials used to produce specimens and Boğaziçi University Construction Materials Lab. personnel Ümit Melep for his most sincere efforts during experiments.

References

- [1] Rodriguez O.G., Hooton R.D., Influence of cracks on chloride ingress into concrete, *ACI Materials Journal*, 100(2), 120-126, 2003.
- [2] Win P.P., Watanabe M., Machida A., Penetration profile of chloride ion in cracked reinforced concrete, *Cement and Concrete Research*, 34, 1073-1079, 2004.
- [3] Marsavina L., Audenaert K., Schutter G.D., Faur N. and Marsavina D., Experimental and numerical determination of the chloride penetration in cracked concrete, *Construction and Building Materials*, 23, 264-274, 2009.
- [4] Gowripalan N., Sirivivatnanon V. and Lim C., Chloride diffusivity of concrete cracked in flexure, *Cement and Concrete Research*, 30, 725-730, 2000.

- [5] Schiessl P., Raupach M., Laboratory studies and calculations on the influence of crack width on chloride induced corrosion of steel in concrete, *ACI Materials Journal*, 94(1), 56-62, 1997.
- [6] Song H.W., Lee C.H., Ann. K.Y., Factors influencing chloride transport in concrete structures exposed to marine environments, *Cement Concrete Composites*, 30, 113-121, 2008.
- [7] Boulfiza M., Sakai K., Banthia N., Yoshida H., Prediction of chloride ions ingress in uncracked and cracked concrete, *ACI Materials Journal*, 100(1), 38-48, 2003.
- [8] Aldea C. M., Shah S. P., Karr A., Permeability of cracked concrete, *Materials and Structures*, 32, 370-376, 1999.
- [9] Djerbi A., Bonnet S., Khelidj A., Baroghel-bouny, V., Influence of traversing crack on chloride diffusion into concrete. *Cement and Concrete Research*, 38, 877-883, 2008.
- [10] Wang K., Jansen D.C., Shah S.P., Karr A.F., Permeability study of cracked concrete, *Cement and Concrete Research*, 27, 381-393, 1997.
- [11] Sahmaran M., Effect of flexure induced transverse crack and self-healing on chloride diffusivity of reinforced mortar, *Journal of Materials Science*, 42, 9131-9136, 2007.
- [12] Wang H., Lu C., Jin W., Bai Y., (2001) Effect of external loads on chloride transport in concrete, *Journal of Materials in Civil Engineering*, 23(7), 1043-1099, 2011.
- [13] Papa N.F., Yinghua Y., Bo D., Effects of crack width on chloride penetration and performance deterioration of RC columns with sustained eccentric compressive load, *KSCCE Journal of Civil Engineering*, 22(2), 637-646, 2018.
- [14] Chunhua L, Jinmu Y, Hui L, Ronggui L., Experimental studies on chloride penetration and steel corrosion in cracked concrete beams under drying-wetting cycles, *Journal of Materials in Civil Engineering*, 29(9), 2017:04017114.
- [15] Beeby A., Corrosion of reinforcing steel in concrete and its relation to cracking, *Structural Engineer Part A*, 56A(3), 77-81, 1978.
- [16] Arya C. and Ofori-Darko F.K., Influence of crack frequency on reinforcement corrosion in concrete, *Cement and Concrete Research*, 26(3), 345-353, 1996.
- [17] Mohammed T.U., Otsuki N., Hamada H., Oxygen permeability in cracked concrete reinforced with plain and deformed bars, *Cement and Concrete Research*, 31, 829-834, 2001.
- [18] Mohammed T.U., Otsuki N., Hisada M., Shibata T., Effect of crack width and bar types on corrosion of steel in concrete, *Journal of Materials in Civil Engineering*, 13, 194-201, 2001.
- [19] Ye H., Jin N., Jin X. and Fu C., Model of chloride penetration into cracked concrete subject to drying-wetting cycles, *Construction and Building Materials*, 36, 259-269, 2012.

- [20] Otieno M, Beushausen H, Alexander M., Towards incorporating the influence of cover cracking on steel corrosion in RC design codes: the concept of performance-based crack width limits, *Materials and Structures*, 45, 1805-1816, 2012.
- [21] Berrocal C.G., Löfgren I., Lundgren K, Tang L, Corrosion initiation in cracked fiber reinforced concrete: Influence of crack width, fiber type and loading conditions, *Corrosion Science*, 98, 128-139, 2015.
- [22] Zafar I, Sugiyama T, The influence of bending crack on rebar corrosion in fly ash concrete subjected to different exposure conditions under static loading, *Construction and Building Materials*, 160, 293-307, 2018.
- [23] Yongsheng J, Yijie H, Lingle Z, Zhongzheng B, Laboratory studies on influence of transverse cracking on chloride induced corrosion rate in concrete, *Cement and Concrete Composites*, 69, 28-37, 2016.
- [24] Sangoju B, Gettu R, Bharkumar B.H, Neelamegam M, Chloride induced corrosion of steel in cracked OPC and PPC concretes: Experimental study, *Journal of Materials in Civil Engineering*, 23(7), 1057-1066, 2011.
- [25] Granju J.L., Balouch S.U., Corrosion of steel fiber reinforced concrete from the cracks, *ACI Materials Journal*, 35, 572-577, 2005.
- [26] Berrocal C.G., Lundgren K., Lofgren I., Influence of steel fibers on corrosion of reinforcement in concrete in chloride environments: A review, *Fiber Concrete 2013*, Prague, Czech Republic, Sept. 12-13, 2013.
- [27] Hay R, Ostertag C.P, Influence of transverse cracks and interfacial damage on corrosion of steel in concrete with and without fiber hybridization, *Corrosion Science*, 153, 213-224, 2019.
- [28] ACI Committee 224R., Control of cracking in concrete structures, *ACI 224-01*, American Concrete Institute, Detroit, Michigan, 2001.
- [29] ACI Committee 318, (2008) Building code requirements for reinforced concrete, *ACI 318-08*, American Concrete Institute, Detroit, Michigan, 2008.
- [30] Bentur A., Diamond S., Berke N.S., Steel corrosion in concrete: Fundamentals and civil engineering practice, *E & FN Spon*, London, United Kingdom, 1997.
- [31] Baah P., Cracking behavior of structural slab bridge decks, *Ph.D. Thesis*, University of Akron, Ohio, 2014.
- [32] ASTM Standard C39/C39M, Standard test method for compressive strength of cylindrical concrete specimens, *ASTM International*, West Conshohocken, PA., 2014.
- [33] ASTM Standard C876, Standard test method for corrosion potentials of uncoated reinforcing steel in concrete, *ASTM International*, West Conshohocken, PA, 2015.
- [34] ASTM Standard C1556. Standard test method for determining the apparent chloride diffusion coefficient of cementitious mixtures by bulk diffusion, *ASTM International*, West Conshohocken, PA., 2017.

- [35] ASTM Standard C1152., Standard test method for acid-soluble chloride in mortar and concrete, *ASTM International*, West Conshohocken, PA.,2012
- [36] ASTM Standard G3, Standard practice for conventions applicable to electrochemical measurements in corrosion testing, *ASTM International*, West Conshohocken, PA, 2017
- [37] Frolund T., Klinghoffer O., Poulsen E., Rebar corrosion rate measurements for service life estimates, *ACI Fall Convention*, Toronto, Canada, 2000.
- [38] Gerard B., Marchand J., Influence of cracking on the diffusion properties of cement-based materials Part I: Influence of continuous cracks on the steady-state regime, *Cement and Concrete Research*, 30, 37-43, 2000.

